You might find this additional info useful...

This article cites 33 articles, 15 of which can be accessed free at:
http://ajprenal.physiology.org/content/293/2/F476.full.html#ref-list-1

This article has been cited by 6 other HighWire hosted articles, the first 5 are:

Epitope-Tagged *Pkhd1* Tracks the Processing, Secretion, and Localization of Fibrocystin
Jason L. Bakeberg, Rachaneekorn Tammachote, John R. Woollard, Marie C. Hogan, Han-Fang
Tuan, Ming Li, Jan M. van Deursen, Yanhong Wu, Bing Q. Huang, Vicente E. Torres, Peter C.
Harris and Christopher J. Ward
JASN, December , 2011; 22 (12): 2266-2277.
[Abstract] [Full Text] [PDF]

**The transcription factor HNF1α regulates expression of chloride-proton exchanger ClC-5
in the renal proximal tubule**
Karo Tanaka, Sara Terryn, Lars Geffers, Serge Garbay, Marco Pontoglio and Olivier Devuyst
Am J Physiol Renal Physiol, December , 2010; 299 (6): F1339-F1347.
[Abstract] [Full Text] [PDF]

**INK4a knockout mice exhibit increased fibrosis under normal conditions and in response
to unilateral ureteral obstruction**
Jesse M. Wolstein, David H. Lee, Jennine Michaud, Venessa Buot, Beth Stefanchik and
Matthew D. Plotkin
Am J Physiol Renal Physiol, December , 2010; 299 (6): F1486-F1495.
[Abstract] [Full Text] [PDF]

**Tubular cell-enriched subpopulation of primary renal cells improves survival and
augments kidney function in rodent model of chronic kidney disease**
Rusty Kelley, Eric S. Werdin, Andrew T. Bruce, Sumana Choudhury, Shay M. Wallace, Roger
M. Ilagan, Bryan R. Cox, Patricia Tatsumi-Ficht, Elias A. Rivera, Thomas Spencer, H. Scott
Rapoport, Belinda J. Wagner, Kelly Guthrie, Manuel J. Jayo, Timothy A. Bertram and Sharon C.
Presnell
Am J Physiol Renal Physiol, November , 2010; 299 (5): F1026-F1039.
[Abstract] [Full Text] [PDF]

**CLC-5 and KIF3B interact to facilitate CLC-5 plasma membrane expression, endocytosis,
and microtubular transport: relevance to pathophysiology of Dent's disease**
Anita A. C. Reed, Nellie Y. Loh, Sara Terryn, Jonathan D. Lippiat, Chris Partridge, Juris
Galvanovskis, Siân E. Williams, Francois Jouret, Fiona T. F. Wu, Pierre J. Courtoy, M. Andrew
Nesbit, Patrik Rorsman, Olivier Devuyst, Frances M. Ashcroft and Rajesh V. Thakker
Am J Physiol Renal Physiol, February , 2010; 298 (2): F365-F380.
[Abstract] [Full Text] [PDF]

Updated information and services including high resolution figures, can be found at:
http://ajprenal.physiology.org/content/293/2/F476.full.html

Additional material and information about *AJP - Renal Physiology* can be found at:
http://www.the-aps.org/publications/ajprenal

This infomation is current as of December 20, 2011.

A primary culture of mouse proximal tubular cells, established on collagen-coated membranes

Sara Terryn,[1,4] François Jouret,[5] Frank Vandenabeele,[2,3] Inge Smolders,[1,3] Marjan Moreels,[2,3] Olivier Devuyst,[3] Paul Steels,[1,3] and Emmy Van Kerkhove[1,4]

[1]*Laboratory of Cell Physiology and* [2]*Laboratory of Histology, Hasselt University and Transnationale Universiteit Limburg,* [3]*Biomedical Institute and* [4]*Centre for Environmental Sciences, Diepenbeek, Belgium; and* [3]*Division of Nephrology, Université Catholique de Louvain, Brussels, Belgium*

Terryn S, Jouret F, Vandenabeele F, Smolders I, Moreels M, Devuyst O, Steels P, Van Kerkhove E. A primary culture of mouse proximal tubular cells, established on collagen-coated membranes. *Am J Physiol Regul Integr Comp Physiol* 293: F476–F485, 2007. First published May 2, 2007; doi:10.1152/ajprenal.00363.2006.—A simple method is described to establish primary cultures of kidney proximal tubule cells (PTC) on membranes. The permeable membranes represent a unique culture surface, allowing a high degree of differentiation since both apical and basolateral membranes are accessible for medium. Proximal tubule (PT) segments from collagenase-digested mouse renal cortices were grown for 7 days, by which time cells were organized as a confluent monolayer. Electron microscopic evaluation revealed structurally polarized epithelial cells with numerous microvilli, basolateral invaginations, and apical tight junctions. Immunoblotting for markers of distinct parts of the nephron demonstrated that these primary cultures only expressed PT-specific proteins. Moreover immunodetection of distinct components of the receptor-mediated endocytic pathway and uptake of FITC-albumin indicated that these cells expressed a functional endocytotic apparatus. In addition, primary cultures possessed the PT brush-border enzymes, alkaline phosphatase, and γ-glutamyl-transferase, and a phloridzin-sensitive sodium-dependent glucose transport at their apical side. Electrophysiological measurements show that the primary cultured cells have a low transepithelial resistance and high short-circuit current that was completely carried by Na^+ similar to a leaky epithelium like proximal tubule cells. This novel method established well-differentiated PTC cultures.

aquaporin; electrophysiological characteristics; phloridzin; receptor-mediated endocytosis; sodium-dependent glucose transport; Ussing chamber

RENAL CELL CULTURE REMAINS an essential tool to investigate kidney cell function (3), transport processes, as well as a variety of cytotoxic (11) or ischemic effects (26) under well-defined conditions. Moreover, the increasing use of knockout or transgenic mouse models needs in vitro evaluation of the cellular phenotype of these animals (2). Up until now, primary cultures of mouse proximal tubular cells (PTC) have been established on solid supports, which allow the access only to the apical side of the cells. Also, previously established techniques used to obtain PTC, like microdissection of individual nephron segments (15) or enzymatic dissection of the kidney (31), are time consuming, have low yields of starting material, and expose the cells to oxidative or mechanical aggression that influence cell differentiation. Primary cultures kept their dif-ferentiated properties until *day 14* in culture, as indicated by the decreased expression of alkaline phosphatase. Dedifferentiation of primary cultures is a well-known phenomenon.

Our goal was to establish a simple and fast method without aggressive manipulations to culture PTC and preserve a high level of differentiation. In contrast to conventional techniques, in which cell cultures were initiated on solid, impermeable cell growth supports, like plastic or glass, we used permeable collagen-coated membrane filter supports. The major advantage of these supports is that epithelial cells, like PTC, can be grown and studied in a polarized state, both the apical and the basolateral sides being accessible and exposed to physiological saline. Doing so, cells can take up and/or secrete molecules on both their apical and basolateral surfaces, resulting in cells that morphologically and functionally better represent their in vivo counterparts. Furthermore, electrophysiological characteristics of PTC grown on permeable filters can be assessed in an Ussing-type chamber.

MATERIALS AND METHODS

Chemicals. Dulbecco's modified Eagle's/Ham's F12 (DMEM-F12) without phenol red, Hank's balanced salt solution (HBSS) without phenol red (liquid, 1×), nonessential amino acids (liquid, 100×), sodium pyruvate, L-glutamine, and penicillin/streptomycin were purchased from Invitrogen Life Technologies (Paisley, Scotland). HEPES and mannitol were obtained from Acros Organics (Geel, Belgium). D-glucose and nylon strainer were obtained from Merck Eurolab (Leuven, Belgium). Collagenase class 2 was purchased from Worthington Biochemical (Lakewood, NJ). [^{14}C]-α-methyl-D-glucopyranoside (α-MG), specific activity of 301 mCi/mmol, was obtained from Amersham Biosciences UK Limited (Buckinghamshire, UK). FITC-labeled bovine serum albumin was purchased from Molecular Probes Europe BV (Leiden, The Netherlands). All other hormones and chemicals were purchased from Sigma (St. Louis, MO). Bio-Rad protein assay was obtained from Bio-Rad Laboratories (Hercules, CA).

Cell culture inserts were 0.33 cm^2 collagen-coated polytetrafluoroethylene (PTFE) membranes, pore size 0.4 μm, and accessory tissue culture-treated cell culture plates were obtained from Corning Costar (Cambridge, MA). Plastic Thermanox coverslips were obtained from Electron Microscopy Sciences (Hatfield, PA).

Primary cell culture. Primary PTC were cultured under sterile conditions from collagenase-digested cortical fragments of kidneys isolated from male C57/BL6-mice (21–30 days) by a modification of previously described methods (15, 26). The C57/BL6 background was chosen, since these mice are mostly used for genetic manipulations.

Renal cortices were dissected visually in ice-cold dissection solution (DS) (HBSS with in mmol/l: 10 glucose, 5 glycine, 1 alanine, 15 HEPES, pH 7.4 and osmolality 325 mosmol/kgH$_2$O) and sliced into pieces of ~1 mm wide. The fragments were transferred to collagenase solution [DS with 0.1% (wt/vol) type-2 collagenase and 96 μg/ml soybean trypsin inhibitor] at 37°C and digested for 30 min. After digestion, the supernatant was sieved through two nylon sieves (pore size 250 μm and 80 μm). Different sieves with pore sizes ranging from 50 to 110 μm were used. Only the 80-μm sieve yielded a large number of long proximal tubule (PT) fragments (about 100 μm in length) without substantial contamination of other nephron segments or glomeruli. The 50-μm sieve used before in our lab to purify medullary thick ascending limbs (15) was not optimal since it retained too many glomeruli. The longer PT fragments remained in the 80-μm sieve and were resuspended by flushing the sieve in the reverse direction with warm DS (37°C) containing BSA 1% (wt/vol). The PTs present in the BSA solution were centrifuged for 5 min at 170 *g*, washed, and then resuspended into the appropriate amount of culture medium: 1:1 DMEM/F12 without phenol red and supplemented with heat-inactivated FCS 1%, HEPES 15 mmol/l, L-glutamine 2 mmol/l, hydrocortisone 50 nmol/l, insulin 5 μg/ml, transferrin 5 μg/ml, selenium 50 nmol/l, sodium pyruvate 0.55 mmol/l, 100× nonessential amino acids 10 ml/l, penicillin 100 IU/ml and streptomycin 100 μg/ml buffered to pH 7.4 and osmolality of 325 mosmol/kgH$_2$O. The PT fragments were seeded onto collagen-coated permeable PTFE-filter supports and left unstirred for 48 h at 37°C and 95% air-5% CO$_2$ in a standard humidified incubator (Jouan, Winchester, VA), after which the culture medium was changed for the first time. The medium was then replaced every 2 days. After 7 days, cell cultures were organized as a confluent monolayer. PTC were also grown on plastic Thermanox coverslips under the same culture conditions for transmission electron microscopy to evaluate whether the morphology was different from cells grown on PTFE-filter supports.

Transmission electron microscopy. The cell-seeded coverslips and support membranes were fixed overnight in a solution of 2% glutaraldehyde in 0.05 mol/l cacodylate buffer (pH 7.3) at 4°C, postfixed in 2% osmium tetroxide in 0.05 mol/l sodium cacodylate buffer (pH 7.3) for 1 h, stained with 2% uranyl acetate in 10% acetone for 20 min, dehydrated in graded concentrations of acetone and routinely embedded in epoxy resin (Araldite). Semithin sections (0.5 μm) were stained with a solution of thionin and methylene blue (0.1% aqueous solution) for light microscopy. Serial ultrathin sections (60 nm) of PTC were mounted on 0.7% formvar-coated grids, contrasted with uranyl acetate and lead citrate and examined with a Philips EM 208 transmission electron microscope operated at 80 kV.

Immunoblotting. The protocol used for immunoblotting has been described previously (10). Cells from 7-day-old primary cultures were harvested by trypsinization, pooled (12 wells/sample) and centrifuged for 10 min at 1,000 *g*. The supernatant was discarded, and the pellet was washed with PBS. After another centrifugation, the pellet was snap-frozen in liquid nitrogen and stored at −80°C until further use. Frozen pellets were solubilized in ice-cold lysis buffer containing protease inhibitors (Complete Mini; Roche Diagnostics, Leuven, Belgium), briefly sonicated (Branson Sonifier 250, two pulses at 40% intensity), and then centrifuged at 16,000 *g* for 1 min at 4°C. The supernatant was transferred into tubes containing 10% SDS and heated at 95°C for 90 s. Protein extracts were separated by SDS-polyacrylamide gels and transferred to nitrocellulose. After blocking, membranes were incubated overnight at 4°C with the first antibody, washed, incubated with peroxidase-labeled secondary antibody, and visualized with enhanced chemiluminescence. For reprobing, the membranes were rinsed, incubated for 30 min at 55°C in a stripping buffer (62.5 mmol/l Tris·HCl, 2% SDS, 100 mmol/l mercaptoethanol, pH 7.4), before incubation with primary antibodies. The signal obtained on membrane extracts from an adult C57/BL6 mouse kidney was used as a positive control. All immunoblots were performed in duplicate.

Immunostaining. After permeabilizing with Triton, 7-day-old confluent monolayers of primary cultured PTC were incubated with 3% BSA for 1 h before adding the primary antibody diluted in PBS that contained 3% BSA. After washing in PBS, cultures were incubated successively with biotinylated secondary anti-IgG antibodies, avidin-biotin peroxidase and aminoethylcarbazole or diaminobenzidine (Vector Laboratories, Burlingame, CA). Sections were viewed under a Nikon Eclipse 80i (Nikon, Tokyo, Japan). The specificity of immunostaining was tested by incubation in the absence of primary antiserum. The quality of the immunostaining is not optimal due to interference of the filter, which can be observed by the striped aspect on the image. Furthermore, the filter is not flat but a wavy surface, and therefore it is difficult to obtain a good focus of all cells of the monolayer. These aspects make these filters less suited for histological purposes compared with glass coverslips or Thermanox.

Antibodies. Immunoblotting and immunostaining analyses were performed using well-characterized sheep polyclonal antibodies against megalin (a gift from P. Verroust, Paris, France) (7); rabbit affinity-purified polyclonal antibodies raised against the NH$_2$ terminus of the human ClC-5 (33); NaCl cotransporter (NCC; a gift from J. Loffing, Lausanne, Switzerland) (18); AQP1 (Chemicon, Temecula, CA); AQP2 (Alomone Labs, Jerusalem, Israël); and sodium-dependent glucose cotransporter type 1 (SGLT1; Abcam, Cambridge, UK) and SGLT2 (Gentaur, Brussels, Belgium); mouse monoclonal antibodies against the 31 kDa E1-subunit (V1 domain) of the V-ATPase (a gift from Dr. S. Gluck, University of California, San Francisco, CA) (5); and β-actin (Sigma, St. Louis, MO).

Uptake of albumin. Uptake of albumin was assessed as described previously (25). Primary PTC were incubated with FITC-labeled bovine serum albumin in Ringer solution for 15 min at 37°C or 4°C as indicated. After rinsing with ice-cold Ringer's solution, cells were disintegrated with Triton X-100 (0.1% vol/vol in Ringer solution). Intracellular fluorescence was measured using a single-beam fluorimeter (Photon Technology International, Lawrenceville, NY), at an excitation wavelength of 480 nm and emission wavelength at 520 nm. Protein concentration was determined by the Bradford protein assay (4).

Alkaline phosphatase assay and γ-glutamyl-transferase assay. The expression of the PT brush border enzyme, alkaline phosphatase, was assessed spectrophotometrically by the two-point method of Walter and Schütt (32). Enzyme activity was standardized to protein concentrations in the cultures or in freshly isolated proximal tubules (isolated PT) measured by the Bradford protein assay (4). Values obtained from 7-day-old cultures were compared with those of 14-day-old cultures and isolated PT, which resemble more closely the in vivo situation since they retain their tubular morphology. To test the adequacy of the method, Madin-Darby canine kidney (MDCK) cells were used as a negative control. MDCK cells are an established cell line derived from distal tubule or cortical collecting duct from the dog and are therefore expected to have a low alkaline phosphatase activity.

In 7-day-old confluent primary cell cultures and isolated PT, the expression of the brush-border enzyme, γ-glutamyl transferase, was assessed by the method described by Glossmann et al. (13). Cell cultures and isolated PT were incubated with γ-glutamyl-*p*-nitroanilide in the presence of MgCl$_2$ and glycylglycine in Tris-buffer (0.05M), and the release of γ-glutamyl-*p*-nitroaniline was measured spectrophotometrically. Enzyme activity was normalized to protein concentrations in the cultures or isolated PT, as measured by the Bradford protein assay (4). One unit of γ-glutamyl-transferase (γ-GT) activity was defined as the amount of enzyme that released 1 μmol of *p*-nitroaniline per unit time at 37°C.

Assessment of Na$^+$-dependent glucose transport. [^{14}C]-α-methyl-D-glucopyranoside (α-MG), a nonmetabolizable glucose analog, was used to study Na$^+$-glucose cotransport in primary PT cells. Seven-day-old confluent cultures were washed 3 times with standard transport buffer (containing in mM: 137 NaCl, 5.4 KCl, 1.2 MgSO$_4$, 2.5 CaCl$_2$, 10 HEPES, and 4.0 L-glutamine buffered to pH 7.4 with

Tris-base and osmolality of 325 mosmol/kgH$_2$O with mannitol). To initiate uptake, transport buffer, containing 20 µCi/ml [^{14}C]α-MG, was added at the apical side of the culture. At the basolateral side, standard transport buffer without tracer was added. After the appropriate time of incubation (5, 30, or 60 min), the uptake was stopped by aspirating the apical solution, and the cells were washed rapidly with ice-cold stop solution (standard transport buffer containing 200 µM phloridzin at 4°C). After the final wash, cells were solubilized with 0.1 N NaOH, and aliquots were sampled for liquid scintillation counting and total protein determination (Bradford protein assay; Ref. 4). To assess the Na$^+$-dependence of the transport, NaCl was replaced with choline chloride (137 mM) in the standard transport buffer. Phloridzin sensitivity was determined by adding 200 µM of phloridzin to the apical transport buffer containing NaCl, while standard transport buffer without phloridzin was added to the basolateral side. To test cell polarity, a radioactive tracer was also added at the basolateral side, and uptake was assessed. All uptake studies were performed at 37°C. Values were expressed in picomoles of α-MG taken up per milligram of proteins.

Measurement of short-circuit current, transepithelial conductance, and capacitance in an Ussing chamber. To perform electrophysiological measurements, we mounted 7-day-old confluent primary cultures grown on permeable filters in a home-built Ussing-type chamber and short-circuited using a high-speed voltage-clamp technique, according to the method described by Van Driessche et al. (30). During the measurements, cultures were constantly perfused at both sides with warm (37°C) Ringer solution (containing in mM: 138 NaCl, 5.33 KCl, 0.41 MgSO$_4$, 1.26 CaCl$_2$, 0.44 KH$_2$PO$_4$, 0.5 MgCl$_2$, 24 HCO$_3$, 10 HEPES, 4 L-glutamine, 5 glycine, 1 alanine, 5.6 D-glucose at pH 7.4 and 325 mosmol/kgH$_2$O) and continuously bubbled with 1% CO$_2$ and 99% air. In Na$^+$-free Ringer, Na$^+$ was replaced with equimolar concentrations of *N*-methyl-D-glucamine, (NMDG), while in glucose-free Ringer, glucose was replaced with the same concentration of sucrose. Both the apical and basolateral solutions were changed to

Fig. 1. Morphologic characteristics of primary proximal tubule cells (PTC) on polytetrafluoroethylene (PTFE) filter. *A*: LM image showing a confluent monolayer of cells at *day 7*. *B*: transmission electron microscopy (TEM) image of cobblestone-like cells grown on a collagen-coated filter (Filter). Scale bar: 10 µm. *C*: TEM image showing the presence of apical microvilli (MV), numerous mitochondria (M), and apical tight junctions (TJ). Scale bar: 2,000 nm. *D*: detail of TEM image showing a vacuole (V) associated with the apical membrane and a tight junction (TJ). Also the basolateral infolds (BI) are clearly visible. Scale bar: 1,000 nm. *E*: detail of TEM image showing a vacuole (V) and a coated vesicle (CV), both associated with the apical cell membrane. Tight junctions (TJ) connect the cells at their apical poles. Scale bar: 1,000 nm. *F*: detail TEM image of a primary cilium (PC) at the apical membrane and the nucleus (N) with heterochromatin. Scale bar: 1,000 nm. *G*: detail of a basolateral invagination (BI). Scale bar: 500 nm.
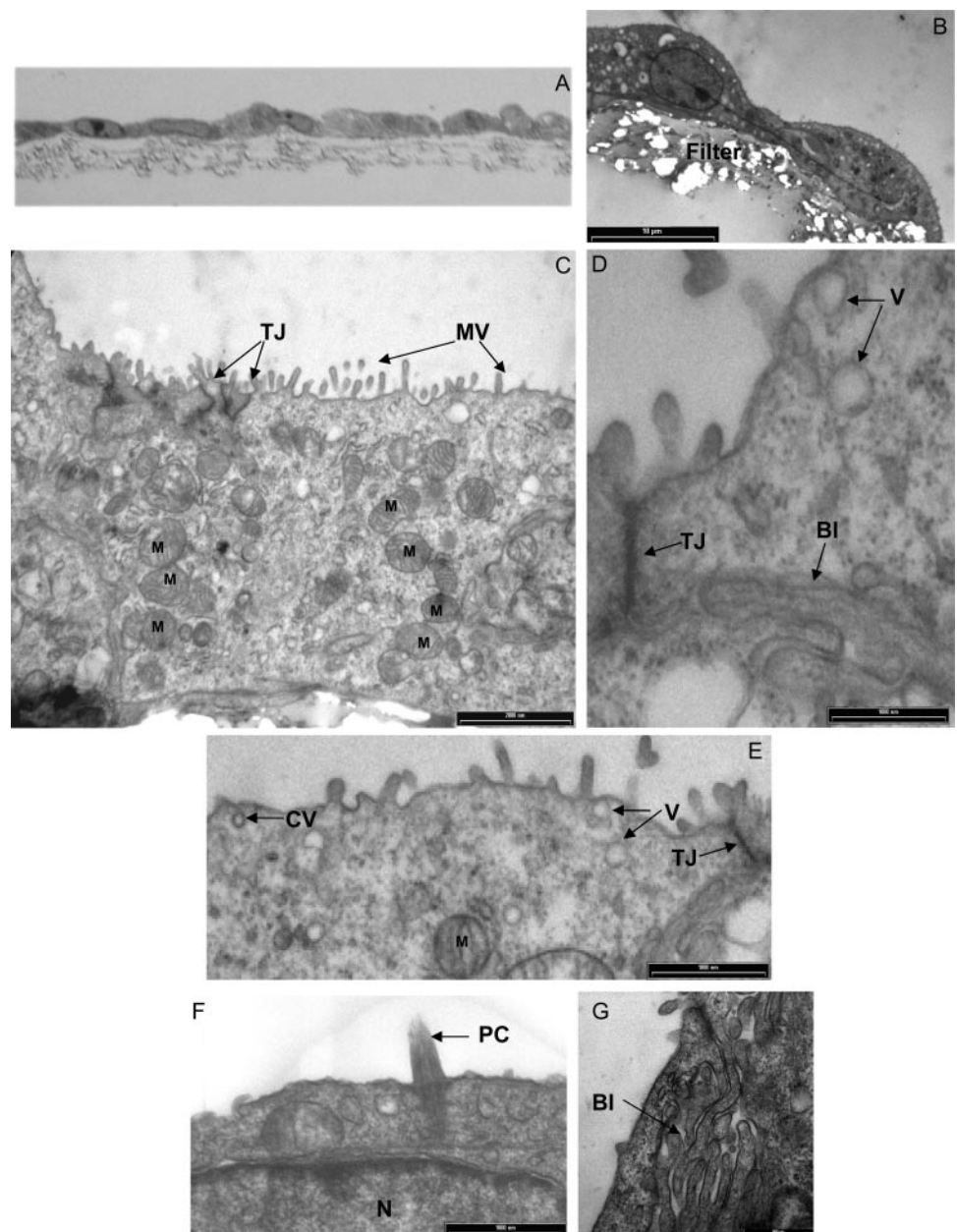
prevent backleak of Na^+ or glucose into the apical compartment. For both Ringer solutions, pH and osmolality were kept similar as control Ringer solution at pH 7.4 and 325 mosmol/kgH$_2$O.

Data. All values are expressed as means ± SE. Data from control experiments were fitted with Origin 6.0 (Micoral Software, Northampton, MA) using the best-fit function. For the albumin uptake experiments, data were fitted according to the Michaelis-Menten kinetics. Significance of differences between two means was calculated using the GraphPad InStat software (demo version, GraphPad Software, San Diego, CA). For the alkaline phosphatase and γ-glutamyl transferase experiments, significance was calculated with one-way ANOVA with Bonferroni correction. For the glucose uptake experiments, significance was calculated by the Kruskal-Wallis test (nonparametric ANOVA) with the Dunn's multiple comparison test. Significance level of the differences of the means is indicated in the legend of each figure.

RESULTS

Primary cell culture. Each cell culture was initiated from the isolation of PT fragments from two kidneys (one mouse). The amount of collected tubules was usually sufficient for 12 collagen-coated PTFE-filter supports. First, PT fragments were left unstirred for 48 h. At this time, cellular outgrowth was observed at the open ends of the tubular fragments. After 7 days, islands of cellular outgrowth became progressively larger to form a confluent monolayer of (epithelial) polygonal cells.

Transmission electron microscopy. At low magnification, the transverse section revealed that single cells grew as a homogeneous monolayer of cells with cobblestone-like appearance on the PTFE filter (Fig. 1, *A* and *B*). The cells were structurally polarized: the apical pole, facing the free surface, differed from the basal pole, toward the underlying support layer. We observed that the apex of the cells exhibited numerous short, regularly oriented microvilli (Fig. 1*C*). The apical cytoplasm possessed clear vacuoles of varying size, some vacuoles being associated with the apical membrane (Fig. 1*D*). Coated vesicles were regularly found (Fig. 1*E*). Well-defined tight junctions interconnected the cells at their apical poles (Fig. 1*C–E*), whereas the basolateral side of the cells showed membrane invaginations (Fig. 1, *D* and *G*). Mitochondria were diffusely distributed in the cytosol, as observed in primary cultures of medullary thick ascending limb cells (15). Also, a primary cilium was present at the apical membrane (Fig. 1*F*).

When PT cells were grown on Thermanox slides, cellular growth was slower compared with the filter supports, since confluency was not reached after 7 days. Furthermore, cells still showed differentiated characteristics like microvilli, but they lost their epithelial organization (data not shown).

Immunoblotting and immunostaining analysis. Well-characterized antibodies against proximal and distal tubule markers were used to establish the state of differentiation of the primary cultures derived from PT segments (Fig. 2). Immunoreactivity for the water channel, AQP1, showed two specific bands, which correspond to the core (~28 kDa) and the glycosylated (~35–50 kDa) forms of the protein, in all samples. By contrast, no signal was detected in the same samples for the thiazide-sensitive NCC and for AQP2, established markers of the early distal convoluted tubule and the collecting duct, respectively. To further characterize the PT cells, immunoblotting for major components of the receptor-mediated endocytosis was performed. The renal chloride channel, ClC-5, which plays a key role along the endocytic pathway in PT cells (7), was clearly
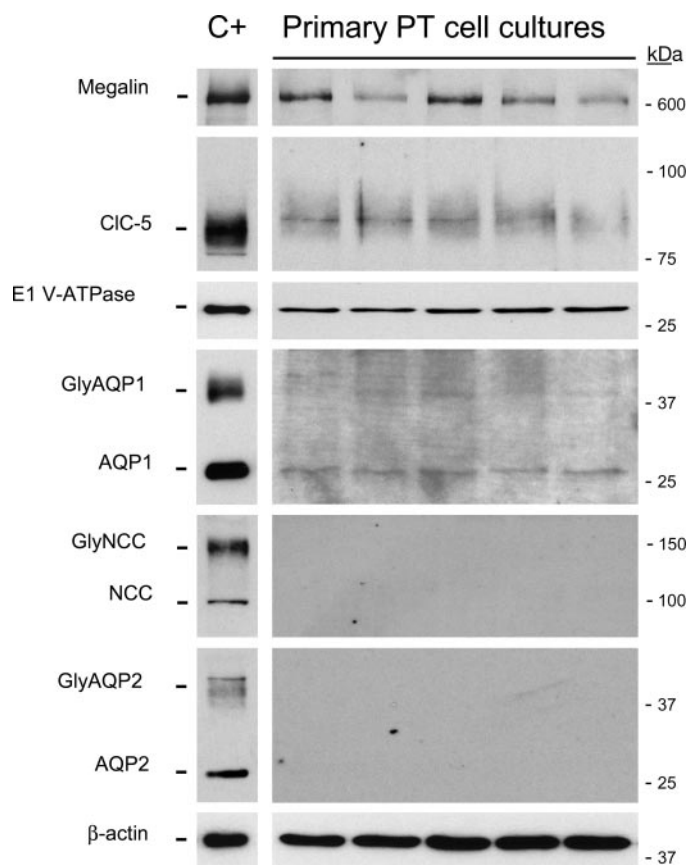

Fig. 2. Representative immunoblottings for proximal tubule (PT), early distal convoluted tubule, and collecting duct markers. Protein extracts from mouse control kidney (C+) and from five pooled 7-day-old primary cultured PT cells (12 wells/sample) were run on SDS-PAGE, transferred to nitrocellulose, and probed with antibodies against megalin (1:4,000), chloride channel-5 (ClC-5; 1:1,000), E1 subunit of the V-type H$^+$-ATPase (V-ATPase; 1:100), aquaporin-1 (AQP1; 1:20,000), NaCl cotransporter (NCC; 1:2,000), and aquaporin-2 (AQP2; 1:1,000). Membranes were stripped and reincubated with a monoclonal antibody against β-actin (1:10,000). In all samples, PT markers, that is, megalin, ClC-5, V-ATPase, and AQP1, are present, whereas no specific signal is detected for NCC and AQP2, even after longer film exposure (up to 2 h).

detected in all samples, as well as its functional partners, the V-ATPase, and the multiligand receptor, megalin. Note that the molecular mass of ClC-5 was slightly higher in cultured PT cells than in the positive control kidney, which might reflect a differential posttranslational processing, e.g., N-glycosylation, of ClC-5 in cultured PT cells (16). Immunoblotting experiments were confirmed by immunostaining on 7-day-old primary PTC (Fig. 3). Almost all cells stained positive for AQP1 (Fig. 3*A*), ClC-5 (Fig. 3*B*), and megalin (Fig. 3*C*), while practically no cells stained for AQP2 (data not shown).

Uptake of albumin. In PTC, albumin is taken up at the apical side by receptor-mediated endocytosis using the multiligand receptors megalin and cubulin (6). The fluorescent probe, FITC-albumin is routinely used to measure receptor-mediated endocytosis and the uptake process is characterized by saturation kinetics. In our cells, uptake of FITC-albumin at 37°C saturates as a function of dose (Fig. 4, ■). Because of the large variability in the analysis, the Lineweaver-Burk plot (Fig. 4, *inset*) for the cell culture sets with lowest uptake data (▲) and highest uptake (●) was assessed. Both experiments, as well as
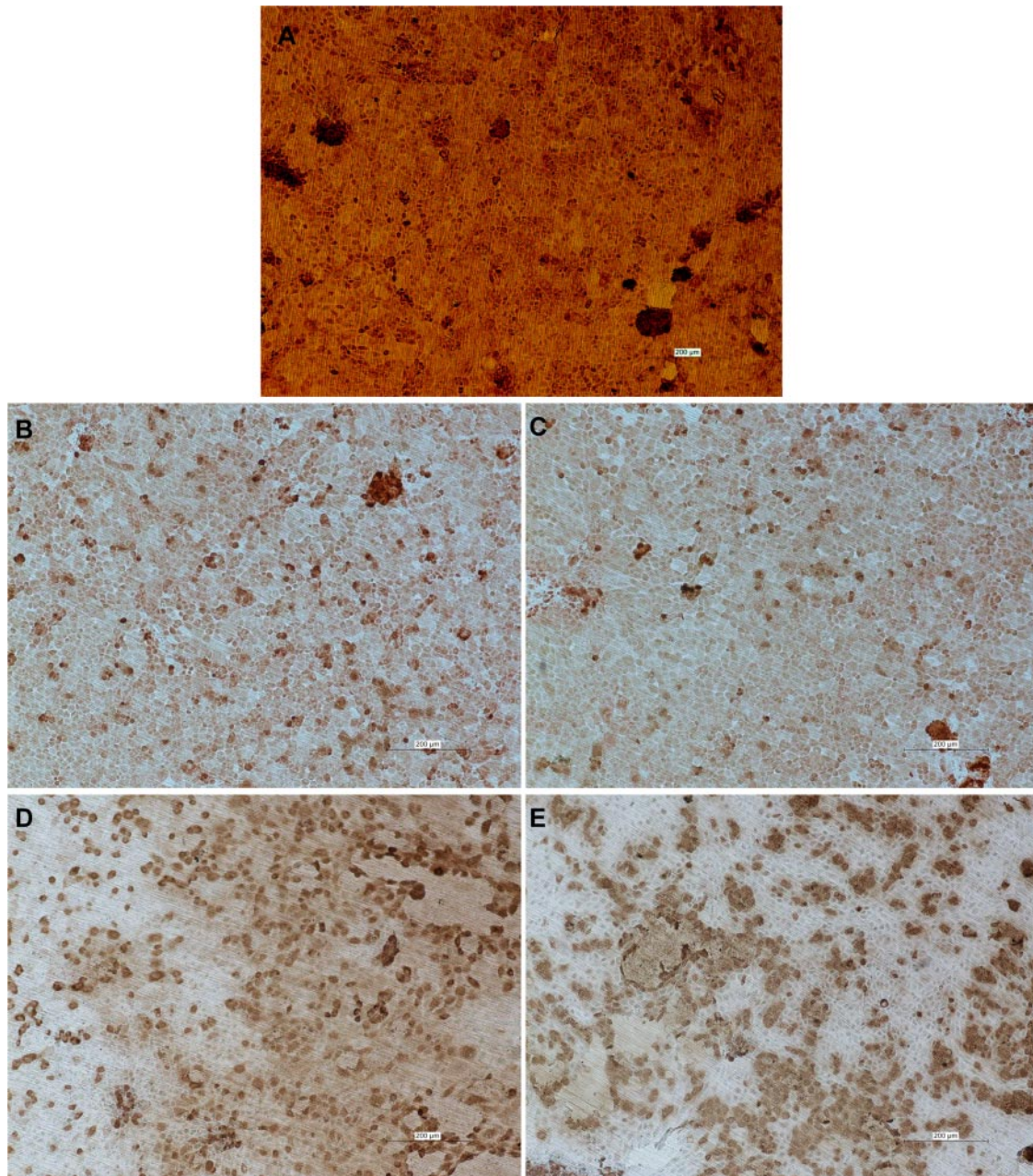
Fig. 3. Immunostaining for AQP1, ClC-5, megalin, SGLT1, and SGLT2 in primary PTC. Immunostaining of 7-day-old primary PTC with primary antibodies raised against AQP1 (*A*), ClC-5 (*B*), megalin (*C*), SGLT1 (*D*) or SGLT2 (*E*). The PTC stained for AQP1, and endocytosis markers, ClC-5 and megalin, as well as the sodium-dependent glucose cotransporter type 1 (SGLT1) and type 2 (SGLT2), while staining for AQP2, a distal tubule marker, was very rare (data not shown). No staining was detected in primary PTC incubated in PBS with 3% BSA without primary antiserum. Magnification: 10× (Scale bar: 200 μm).

the mean (■), have the same apparent K_m (intercept with *x*-axis) but a different V_{max} (intercept with *y*-axis) (Table 1). Using the Michaelis-Menten kinetics (Fig. 4) and the Lineweaver-Burk plot (Fig. 4, *inset*), the mean maximal uptake (V_{max}) was calculated to be 1.5 ± 0.6 ng/μg protein/15 min, and the apparent K_m (concentration for half-maximum uptake) was estimated at 36 ± 0.9 mg/l ($n = 12$). At 4°C, the uptake represents the cell-bound fluorescence and should therefore not rise as a function of dose. Indeed, at this low temperature, the uptake process is delayed and does not rise with higher doses (Fig. 4, ○).

Alkaline phosphatase and γ-glutamyl-transferase assay. Alkaline phosphatase and γGT are enzymes expressed at the brush border of PTC. Their activity can be classically assessed by spectrophotometrical methods based on the color conversion of *p*-nitrophenyl phosphate to *p*-nitrophenol in an alkaline solution or γ-glutamyl-*p*-nitroanilide to the yellowish *p*-nitroaniline, respectively. To localize the enzymes in our cultures, we tested the solution containing *p*-nitrophenyl phosphate or γ-glutamyl-*p*-nitroanilide at both apical and basolateral sides of the cells. Enzyme activity for the apical side is presented in Fig. 5. Enzyme activity was also assessed at the basolateral
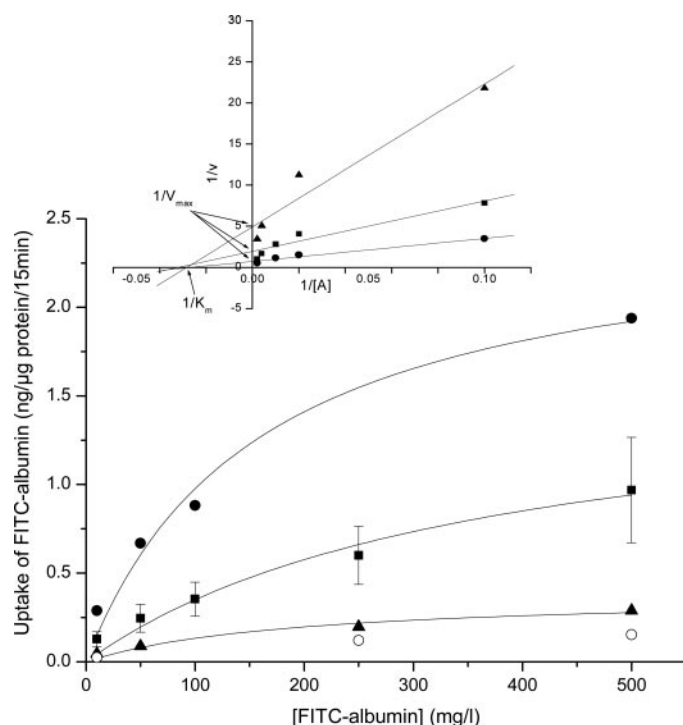
Fig. 4. Uptake of FITC-albumin in primary PTC. Uptake of FITC-albumin assessed in 7-day-old primary PTC at 37°C (■, $n = 12$) and at 4°C (○, $n = 1$) for 15 min. The uptake at 37°C clearly rises as a function of the dose but gradually saturates at higher doses, while at 4°C, there is no dependence on dose. V_{max} was calculated to be 1.5 ± 0.6 ng·μg protein^{-1}·15 min^{-1} and the apparent K_m was 36 ± 0.9 mg/l. The large error in the analysis is due to heterogeneity between different sets of cultures. The uptake data from the culture set with the lowest (▲) and highest (●) uptake are also shown. *Inset*: shows the Lineweaver-Burk plot of the experiment with the lowest (▲) uptake data and the experiment with the highest (●) uptake data. The Lineweaver-Burk plot of the mean uptake is presented by squares. The intercept with the x-axis ($y = 0$) is $1/K_m$ and the intercept with the y-axis ($x = 0$) is $1/V_{max}$. From the three data sets, the $1/V_{max}$ value is different, while the $1/K_m$ value is similar. Each value is the mean $\pm$ SE of the different determinations (n), except for determinations at 4°C and the highest and lowest uptake culture set.

side, but no activity was measured. For alkaline phosphatase, the activity in 7-day-old primary PTC was about 20 times higher than in 14-day-old primary cultures, indicating the degree of differentiation is dependent on time in culture (Fig. 5, open bars). In isolated PT, enzyme activity was about 4 times lower than in primary PTC. To test whether the two-point method (32) that we used was adequate to evaluate the presence of alkaline phosphatase in our culture system, we compared MDCK cells with 7-day-old primary PTC. MDCK cells are from a distal tubular origin and are therefore assumed to have a low alkaline phosphatase activity, as indeed documented here. MDCK cells displayed an alkaline phosphatase activity that was ~5,000 times lower than that of 7-day-old primary PT cells and still ~200 times lower than that of 14-day-old primary PT cells (Fig. 5, open bars). For γ-GT, the activity in 7-day-old primary PTC amounted to 172.5 ± 13.9 mU/mg protein, which was higher than the values reported by Cummings et al. (8) in primary cultures of human proximal tubule cells but lower than the values reported for whole mouse kidney (275 mU/mg protein) (14). In freshly isolated PT, enzyme activity was about 2 times lower than in primary PTC (Fig. 5, striped bars).

Na$^+$-dependent transport of glucose. Transport of glucose is a highly differentiated function of renal PT cells localized at the apical membrane (35). To test whether our primary cells still displayed this function, we evaluated the uptake of [^{14}C]-α-methyl-D-glucopyranoside (α-MG). To localize the transport of glucose, α-MG was tested at both apical and basolateral sides of the cells. When α-MG was added to the basolateral side, we did not observe any uptake into the cells (data not shown). Therefore, we evaluated α-MG uptake under various conditions at the apical side. The addition of unlabeled α-MG to the transport buffer did not affect uptake of labeled α-MG; therefore data presented in Fig. 6 represent uptake of only labeled α-MG. The time course of α-MG uptake was saturable since it slowly reached a maximum transport rate after 60 min (Fig. 6, ■). The addition of phloridzin (200 μM), a competitive inhibitor of glucose reabsorption, resulted in a significant reduction of the α-MG uptake after 30 and 60 min in the presence of Na$^+$ (Fig. 6, ▲). The uptake of α-MG was only 12% of control after 60 min in the presence of phloridzin. When Na$^+$ was omitted from the transport buffer and replaced by an equal amount of choline, uptake of α-MG without Na$^+$ was significantly reduced after 30 and 60 min (Fig. 6, ●). Omission of Na$^+$ reduced transport rates. The maximum rate was only 18% of the control after 60 min. Still a small amount of α-MG was taken up under Na$^+$-free conditions. Immunostaining for the SGLT1 and SGLT2 is shown in Fig. 3 (F+G+L+M). Primary cultures of 7-day-old PTC expressed both SGLT1 and SGLT2.

Electrophysiological characteristics of primary cultured PTC. Cell monolayers were allowed to stabilize to a steady-state level before omitting Na$^+$ or glucose from the control Ringer solution. Steady-state values for the short-circuit current (I_{sc}), transepithelial conductance (G_T) and capacitance (C_T) were determined at 26.85 ± 0.21 μA/cm^2, 14.98 ± 0.03 mS/cm^2, and 0.81 ± 0.005 μF/cm^2, respectively (Fig. 7, $n = 3$). Replacing Na$^+$ for NMDG immediately dropped I_{sc}, while a small drop in G_T (22%) and C_T (3%) was observed (Table 2). When glucose was replaced by sucrose in the Ringer solution also a drop in I_{sc}, G_T and C_T could be observed, although the reduction was much smaller than after replacement of Na$^+$ for NMDG: 10% decrease for I_{sc}, 8% decrease for G_T and 1.2% decrease for C_T (Table 1).

Table 1. *Calculated apparent K_m values and V_{max} values for uptake of albumin from culture sets with high and with low uptake compared to the mean*

Cell Culture Set	Apparent K_m	V_{max}
Mean uptake (Fig. 4, ■)	36 ± 0.9 mg/l	1.5 ± 0.6 ng·μg protein^{-1}·0.15 min^{-1}
Lowest uptake (Fig. 4, ▲)	35 mg/l	0.4 ng·μg protein^{-1}·0.15 min^{-1}
Highest uptake (Fig. 4, ●)	38 mg/l	2.5 ng·μg protein^{-1}·0.15 min^{-1}

Apparent K_m values and V_{max} values calculated from the Lineweaver-Burk plot from different sets of cell cultures as indicated in Fig. 4. Different culture sets had different V_{max} values, but the same apparent K_m value, indicating the presence of the same transport system but a variable level of expression of the transport proteins involved.

Fig. 5. Alkaline phosphatase and γ-glutamyl-transferase activity in primary PTC. Alkaline phosphatase (AP) activity (open bars, left *y*-axis) measured in 7-day-old, 14-day-old primary cultures of PTC, Madin-Darby canine kidney (MDCK) cells and freshly isolated proximal tubules (isolated PT). Values (means $\pm$ SE) are in micromoles per milligram protein per minute: 129.6 ± 26.6, 7.5 ± 3.2, 0.026 ± 0.004, and 33.7 ± 6.6 for 7-day-old PTC ($n = 16$), 14-days old PTC ($n = 4$), MDCK cells ($n = 8$), and isolated PT ($n = 16$), respectively. Each value is the mean of different determinations (n). Significance was determined by one-way ANOVA with Bonferroni correction and *P* values are *$P < 0.001$ and **$P < 0.0001$. Gamma-glutamyl-transferase (γGT) (hatched bars, right *y*-axis) activity was measured in 7-day-old primary cultures of PTC ($n = 21$) and isolated PT ($n = 16$) and amounted to a value (means $\pm$ SE) of 172.5 ± 13.9 mU/mg protein and 82.7 ± 2.9 mU/mg protein, respectively.
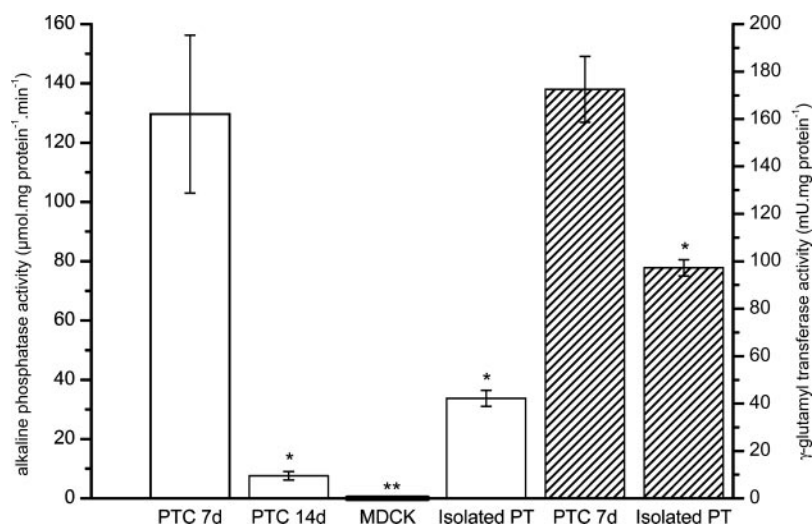
DISCUSSION

Microdissection of individual nephron segments was used to culture PT cells from mouse kidney. The microdissection technique has the major advantage of providing pure starting material (15). However, the yield is rather low, and it is a time-consuming method exposing the cells to oxidative or mechanical aggression. PT cells have been shown to be very susceptible to membrane damage during the isolation method compared with tubular fragments of a more distal origin (31). Thus, to properly culture PT cells, we need a fast isolation method with a minimum of aggressive manipulations.

The method described here is a combination of careful dissection of the kidney, enzymatic digestion and sieving. This low cost procedure is characterized by a rather high yield, and it enables a rapid isolation of a large number of PT fragments. When brought into culture, cellular outgrowth is observed at the open ends of the tubular fragments within a few days. After 7 days, a monolayer of polygonal PTC is formed. Taub et al. (28) reported the use of hormonally defined serum-free medium to culture differentiated PTC, with restricted outgrowth of fibroblasts or glomeruli. In our hands, the absence of serum caused a restricted growth of the PT cultures, and a concentration of 1% FCS was necessary to obtain confluent cultures within a reasonable time. No fibroblast overgrowth was observed.

Electron microscopic analysis revealed that confluent monolayers grown on collagen-coated membranes had a cobblestone-like appearance and were polarized with tight junctions confined to the apical poles. Coated vesicles were also observed in the PTC and are known to be involved in the endocytic uptake mechanism of reabsorption of low-molecular weight proteins that have been filtered across the glomerulus. Moreover, the cytosol contained numerous mitochondria and also basolateral invaginations were observed, both character-
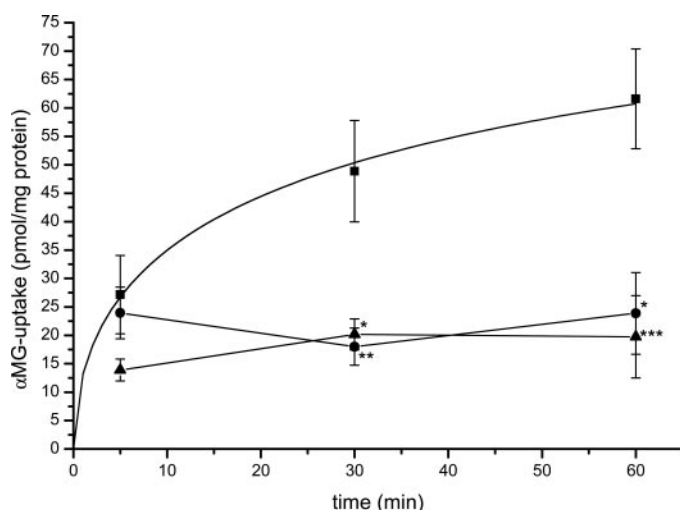

Fig. 6. [^{14}C]-α-methyl-D-glucopyranoside (α-MG) uptake in primary cultures of PTC. The uptake of α-MG reaches a maximum after about 60 min (■). Glucose transport is sensitive to omission of Na$^+$ (●) and can be blocked by phloridzin (▲). Values are means $\pm$ SE; each value is the mean of five to seven determinations. Significance was analyzed by Kruskal-Wallis test (nonparametric ANOVA) with the Dunn's multiple comparisons test and *P* value was *$P < 0.05$, **$P < 0.01$, and ***$P < 0.001$.
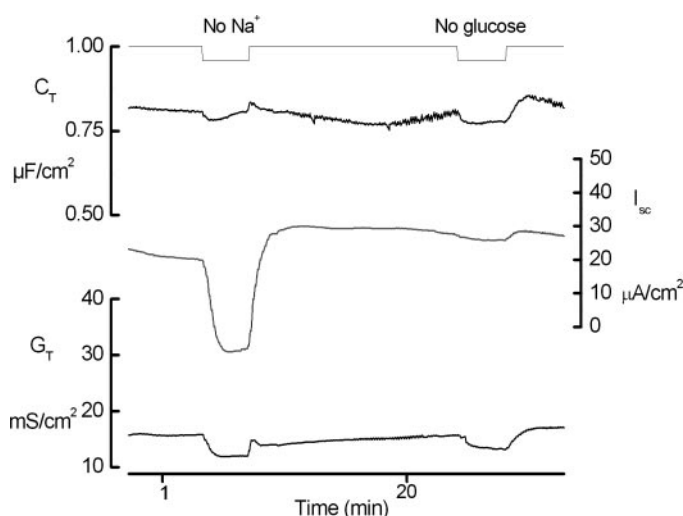

Fig. 7. Electrophysiological characteristics of primary PTC. Time courses for short-circuit current (I_{sc}), transepithelial conductance (G_T), and transepithelial capacitance (C_T) in basal steady-state conditions and after omission of Na$^+$ (No Na$^+$), and glucose (No glucose). Traces represent a representative experiment out of three different measurements from 7-day-old confluent primary PTC.

Table 2. *I_{sc}, G_T, and C_T evolution after Na^+ and glucose omission for control Ringer solution*

	I_{sc}, μA/cm^2	G_T, mS/cm^2	C_T, μF/cm^2
Condition 1			
Basal	21.16 ± 0.1	15.73 ± 0.01	0.82 ± 0.0005
No Na$^+$	$-2.15 \pm 1.1^*$	$12.4 \pm 0.13^*$	0.79 ± 0.001
ΔNo Na$^+$ − basal	23.31 ± 1.0	3.33 ± 0.12	0.03 ± 0.0005
%Decrease	110%	21%	4%
Condition 2			
Basal	29.07 ± 0.04	14.91 ± 0.03	0.79 ± 0.001
No glucose	$26.06 \pm 0.05^*$	$13.78 \pm 0.1^*$	0.78 ± 0.001
ΔNo glucose − basal	3.01 ± 0.01	1.13 ± 0.07	0.01 ± 0.001
%Decrease	10%	8%	1.2%

Short-circuit current (I_{sc}), transepithelial conductance (G_T), and capacitance (C_T) of 7-day-old confluent primary cultures were measured in an Ussing chamber in control conditions (basal), after replacing Na$^+$ for *N*-methyl-D-glucamine (NMDG; No Na$^+$) and after replacing glucose for sucrose (No glucose). Values are expressed as means ± SE; $n = 3$. *$P < 0.001$.

istic features of PTC in vivo. We also show that PTC cultured in our conditions show a primary cilium at the apical membrane, which is another indicator of their differentiation (19). These results indicate that PTC when cultured on permeable collagen-coated filter membranes retain a high degree of morphologic differentiation. By contrast, when grown on a solid support, cells were flatter, and the apical tight junctions were less defined. The PTC developed typical ultrastructural characteristics of myofibroblasts, such as stress fibers.

The presence of specific markers, like transporter proteins or brush-border enzymes, was established to characterize these primary cultures (1). In particular, we evaluated the expression of the PT water channel, AQP1, compared with NCC and AQP2, which are mostly expressed in the early distal tubule and in the collecting duct, respectively. The PTC cultured in our conditions showed a clear immunoreactivity against AQP1, while no positive signal for AQP2 or NCC was obtained. These results indicate that our primary cell cultures originated from PT cells, without significant contamination of cells from other parts of the nephron. Moreover, we investigated whether specific markers of the endocytic apparatus were present in our primary cultures. The multiligand receptor, megalin, is located at the brush border of PT cells and participates in protein reabsorption from the primitive urine. The chloride channel ClC-5 and the vacuolar proton pump V-ATPase are both localized in endosomes (10, 16, 22) ensuring correct endosomal acidification and protein trafficking in PT cells (7). All of these components of the endocytic apparatus were detected in our primary PT cells, indicating that these cells possess functional markers of the PT. Because essential components of the endocytic apparatus were detected in our primary PT cells, we then investigated whether receptor-mediated endocytosis could be performed by these cells. The quantitative analysis of the uptake process of FITC-albumin showed that the uptake was saturable as a function of dose and decreased at 4°C. The calculated apparent K_m (36 ± 0.9 mg/l) was comparable with those described in the literature (12, 17, 20, 25), indicating the presence of a functional endocytic apparatus characterized by a high affinity and low capacity in our cells. The large variability in the analysis is due to the heterogeneity among different sets of cell cultures. Lineweaver-Burk analysis of cell

cultures with high uptake and low uptake compared with mean values (Fig. 4, *inset*) shows that the different sets of cell cultures possess different V_{max} values, but the same K_m value, meaning that the same transport system is present but that the expression levels at the brush-border membrane is different. In the immunoblotting experiments, a difference in level of expression of megalin between different sets of cultures was observed. Therefore, the difference in rate of uptake (different V_{max} values) could be explained by the difference in expression levels of megalin, the receptor responsible for binding and internalizing albumin in proximal tubule cells (6). As all uptake data are normalized for the amount of protein in each cell culture, and all experiments are conducted on 7-day confluent monolayers, we believe that factors like age of cell cultures and cell density, as well as number of cell divisions can be ruled out to play a role in the differences observed in V_{max}.

Thus, the method enables us to isolate and grow highly differentiated primary cultures, which express distinct essential PT transport proteins.

By a simple spectrophotometric assay, we demonstrated the presence of alkaline phosphatase, an enzyme that catalyzes the hydrolysis of phosphate monoesters, and γ-glutamyl-transferase, an enzyme that catalyses the transfer of a γ-glutamyl moiety of glutathione to a variety of α-amino acids. Freshly isolated proximal tubules were also analyzed since they resemble more closely the in vivo situation, so it is expected that enzyme activity is preserved as well. For both enzymes, the activity was lower in isolated PT compared with 7-day-old PTC. This difference might be due to the collapse of the tubular lumen during isolation (21), and therefore, only enzyme activities at the open ends are measured. However, surface markers, like brush-border enzymes, are known to be unstable during the transition from in vivo to in vitro (29). To characterize our cells functionally, we evaluated the transport of glucose at the apical membrane, another specific cellular function of PT cells. PT cells possess at their apical membrane a sodium-dependent glucose transport system (9) ensured by the SGLT-protein (35). Using [^{14}C]-α-methyl-D-glucopyranoside (α-MG), a stable glucose analog transported by SGLT, we demonstrated that our primary cultures were capable of transporting glucose. The uptake of α-MG, strictly observed at the apical side of the cells, was saturable as a function of time and almost completely inhibited by phloridzin, a nontransportable competitive inhibitor of the SGLT proteins as observed by Schaaf et al. (24). When sodium was omitted from the transport buffer and replaced by choline chloride, sugar uptake was only 18% of control values after 60 min, indicating that the observed α-MG transport is indeed sodium dependent. Note that a small amount of α-MG was still taken up in Na$^+$-free conditions, which might represent passive diffusion of α-MG (23). Immunostaining showed the presence of both SGLT1 and SGLT2 in primary PTC. These subtypes of the SGLT family are expressed in different segments of the proximal tubule with SGLT1 being preferentially expressed in the S3 segment and SGLT2 in the S1/S2 segment. In our primary cultures, proximal tubule cells from both segments are present. These results demonstrate the presence of a sodium-dependent glucose transport at the apical membrane of our primary cultured cells.

The major advantage of culturing PTC on permeable supports is that in this way, their electrophysiological character-

istics can be assessed in an Ussing-type chamber. Proximal tubule cells form a leaky epithelium possessing a high transport of Na^+ and a typically low transepithelial resistance (R_T). In our primary cultured PTC, we measured a high I_{sc}, which dropped immediately after replacing Na^+ for NMDG in the Ringer solution, indicating that the current was completely carried by Na^+ and that the Na^+-K^+-ATPase in the basolateral membrane is present and active. After replacing glucose for sucrose in the Ringer solution, a small drop in I_{sc} was observed, indicating that glucose is transported over the apical membrane in an electrogenic way, achieved by the presence of a sodium-dependent glucose cotransporter at the apical membrane. The drop in I_{sc} after glucose omission is smaller than the decrease in I_{sc} after Na^+ deletion. This implies that other electrogenic Na^+ cotransporters are present as well. The R_T was characteristically low (around 66 Ohm/cm^2). These results indicate that our cultured PTCs represent the typical electrophysiological characteristics of a leaky proximal tubule epithelium (34). The small drop in capacitance after omission of Na^+ or glucose might be due to a drop in transport, resulting in a closure of the lateral intercellular spaces, as has been described previously by Van Driessche et al. (30) and Spring and Hope (27).

In conclusion, we have described a novel method to culture mouse PT cells on collagen-coated membranes with a reasonable yield. Electron microscopic analysis displayed a differentiated morphology of polarized cells with characteristics of PT cells. Furthermore, the presence of PT-specific proteins, such as water, ion, or glucose transporters; a receptor-mediated endocytosis of proteins; and efficient brush-border-associated enzymes demonstrated that these primary cells retained the differentiated functions of their in vivo counterparts for at least 3 to 4 days. Electrophysiological analysis revealed that these primary PTCs possessed all typical characteristics of a leaky proximal tubule epithelium with a high Na^+ transport rate. Since these cultures were established on collagen-coated membranes, this method represents a useful tool to study a variety of proximal transport systems, as well as the influences of different substances like hormones at both the apical and the basolateral sides of the PT cell. Moreover, used in an Ussing chamber, the confluent monolayer allows us to study and follow the electrogenic transport characteristics online.

REFERENCES

1. **Agre P, King LS, Yasui M, Guggino WB, Ottersen OP, Fujiyoshi Y, Engel A, Nielsen S.** Aquaporin water channels—from atomic structure to clinical medicine. *J Physiol* 542: 3–16, 2002.

2. **Bell CL, Tenenhouse HS, Scriver CR.** Isolation and culture of murine renal proximal tubule cells: a system to study solute transport in mutants. *Ann NY Acad Sci* 456: 398–400, 1985.

3. **Bello-Reuss E, Weber MR.** Electrophysiological studies on primary cultures of proximal tubule cells. *Am J Physiol Renal Fluid Electrolyte Physiol* 251: F490–F498, 1986.

4. **Bradford MM.** A rapid and sensitive method for the quantitation of microgram quantities of protein utilizing the principle of protein-dye binding. *Anal Biochem* 72: 248–254, 1976.

5. **Brown D, Hirsch S, Gluck S.** Localization of a proton-pumping ATPase in rat kidney. *J Clin Invest* 82: 2114–2126, 1988.

6. **Christensen EI, Birn H.** Megalin and cubilin: multifunctional endocytic receptors. *Nat Rev Mol Cell Biol* 3: 256–266, 2002.

7. **Christensen EI, Devuyst O, Dom G, Nielsen R, Van der Smissen P, Verroust P, Leruth M, Guggino WB, Courtoy PJ.** Loss of chloride channel ClC-5 impairs endocytosis by defective trafficking of megalin and cubilin in kidney proximal tubules. *Proc Natl Acad Sci USA* 100: 8472–8477, 2003.

8. **Cummings BS, Lasker JM, Lash LH.** Expression of glutathione-dependent enzymes and cytochrome *P*-450s in freshly isolated and primary cultures of proximal tubular cells from human kidney. *J Pharmacol Exp Ther* 293: 677–685, 2000.

9. **Del Valle PL, Trifillis A, Ruegg CE, Kane AS.** Characterization of glucose transport by cultured rabbit kidney proximal convoluted and proximal straight tubule cells. In Vitro *Cell Dev Biol Anim* 38: 218–227, 2002.

10. **Devuyst O, Christie PT, Courtoy PJ, Beauwens R, Thakker RV.** Intra-renal and subcellular distribution of the human chloride channel, CLC-5, reveals a pathophysiological basis for Dent's disease. *Hum Mol Genet* 8: 247–257, 1999.

11. **Elliget KA, Trump BF.** Primary cultures of normal rat kidney proximal tubule epithelial cells for studies of renal cell injury. In Vitro *Cell Dev Biol* 27A: 739–748, 1991.

12. **Gekle M, Mildenberger S, Freudinger R, Silbernagl S.** Functional characterization of albumin binding to the apical membrane of OK cells. *Am J Physiol Renal Fluid Electrolyte Physiol* 271: F286–F291, 1996.

13. **Glossmann H, Neville DM.** gamma-Glutamyltransferase in kidney brush border membranes. *FEBS Lett* 19: 340–344, 1972.

14. **Hanigan MH, Gallagher BC, Townsend DM, Gabarra V.** Gamma-Glutamyl transpeptidase accelerates tumor growth and increases the resistance of tumors to cisplatin in vivo. *Carcinogenesis* 20: 553–559, 1999.

15. **Jans F, Vandenabeele F, Helbert M, Lambrichts I, Ameloot M, Steels P.** A simple method for obtaining functionally and morphologically intact primary cultures of the medullary thick ascending limb of Henle's loop (MTAL) from rabbit kidneys. *Pflügers Arch* 440: 643–651, 2000.

16. **Jouret F, Igarashi T, Gofflot F, Wilson PD, Karet FE, Thakker RV, Devuyst O.** Comparative ontogeny, processing, and segmental distribution of the renal chloride channel, ClC-5. *Kidney Int* 65: 198–208, 2004.

17. **Lazzara MJ, Deen WM.** Model of albumin reabsorption in the proximal tubule. *Am J Physiol Renal Physiol* 292: F340–F349, 2007.

18. **Loffing J, Vallon V, Loffing-Cueni D, Aregger F, Richter K, Pietri L, Bloch-Faure M, Hoenderop JG, Shull GE, Meneton P, Kaissling B.** Altered renal distal tubule structure and renal Na(+) and Ca(2+) handling in a mouse model for Gitelman's syndrome. *J Am Soc Nephrol* 15: 2276–2288, 2004.

19. **Pan J, Wang Q, Snell WJ.** Cilium-generated signaling and cilia-related disorders. *Lab Invest* 85: 452–463, 2005.

20. **Park CH, Maack T.** Albumin absorption and catabolism by isolated perfused proximal convoluted tubules of the rabbit. *J Clin Invest* 73: 767–777, 1984.

21. **Rodeheaver DP, Aleo MD, Schnellmann RG.** Differences in enzymatic and mechanical isolated rabbit renal proximal tubules: comparison in long-term incubation. In Vitro *Cell Dev Biol* 26: 898–904, 1990.

22. **Sakamoto H, Sado Y, Naito I, Kwon TH, Inoue S, Endo K, Kawasaki M, Uchida S, Nielsen S, Sasaki S, Marumo F.** Cellular and subcellular immunolocalization of ClC-5 channel in mouse kidney: colocalization with H$^+$-ATPase. *Am J Physiol Renal Physiol* 277: F957–F965, 1999.

23. **Sakhrani LM, Badie-Dezfooly B, Trizna W, Mikhail N, Lowe AG, Taub M, Fine LG.** Transport and metabolism of glucose by renal proximal tubular cells in primary culture. *Am J Physiol Renal Fluid Electrolyte Physiol* 246: F757–F764, 1984.

24. **Schaaf GJ, de Groene EM, Maas RF, Commandeur JN, Fink-Grem-mels J.** Characterization of biotransformation enzyme activities in primary rat proximal tubular cells. *Chem Biol Interact* 134: 167–190, 2001.

25. **Schwegler JS, Heppelmann B, Mildenberger S, Silbernagl S.** Receptor-mediated endocytosis of albumin in cultured opossum kidney cells: a model for proximal tubular protein reabsorption. *Pflügers Arch* 418: 383–392, 1991.

26. **Sheridan AM, Schwartz JH, Kroshian VM, Tercyak AM, Laraia J, Masino S, Lieberthal W.** Renal mouse proximal tubular cells are more susceptible than MDCK cells to chemical anoxia. *Am J Physiol Renal Fluid Electrolyte Physiol* 265: F342–F350, 1993.

27. **Spring KR, Hope A.** Fluid transport and the dimensions of cells and interspaces of living Necturus gallbladder. *J Gen Physiol* 73: 287–305, 1979.

28. **Taub ML, Yang IS, Wang Y.** Primary rabbit kidney proximal tubule cell cultures maintain differentiated functions when cultured in a hormonally defined serum-free medium. In Vitro *Cell Dev Biol* 25: 770–775, 1989.

29. **Van der Biest I, Nouwen EJ, Van Dromme SA, De Broe ME.** Characterization of pure proximal and heterogeneous distal human tubular cells in culture. *Kidney Int* 45: 85–94, 1994.

30. **Van Driessche W, De Vos R, Jans D, Simaels J, De Smet P, Raskin G.** Transepithelial capacitance decrease reveals closure of lateral interspace in A6 epithelia. *Pflügers Arch* 437: 680–690, 1999.

31. **Wagner CA, Lukewille U, Valles P, Breton S, Brown D, Giebisch GH, Geibel JP.** A rapid enzymatic method for the isolation of defined kidney tubule fragments from mouse. *Pflügers Arch* 446: 623–632, 2003.

32. **Walter K, Schütt C.** Acid and alkaline phosphatase in serum (two-point method). In: *Methods of Enzymatic Analysis*, edited by Bergmeyer HU. New York: Academic, 1974, p. 856–864.

33. **Wang SS, Devuyst O, Courtoy PJ, Wang XT, Wang H, Wang Y, Thakker RV, Guggino S, Guggino WB.** Mice lacking renal chloride channel, CLC-5, are a model for Dent's disease, a nephrolithiasis disorder associated with defective receptor-mediated endocytosis. *Hum Mol Genet* 9: 2937–2945, 2000.

34. **Weinstein AM.** Sodium and chloride transport: Proximal nephron. In: *The Kidney: Physiology and Pathophysiology*, edited by Seldin DW and Giebisch G. Philadelphia: Lippincott Williams & Wilkins, 2000, p. 1287–1331.

35. **Wright EM.** Renal Na^+-glucose cotransporters. *Am J Physiol Renal Physiol* 280: F10–F18, 2001.